Copyright ©2007 by the Society for Industrial and Applied Mathematics
This electronic version is for personal use and may not be duplicated or distributed.

Chapter 3

A Basic Model for Tomography

We begin our study of medical imaging with a mathematical model of the measurement process used in x-ray tomography. The model begins with a quantitative description of the interaction of x-rays with matter called Beer's law. In this formulation the physical properties of an object are encoded in a function μ, called the *attenuation coefficient*. This function quantifies the tendency of an object to absorb or scatter x-rays. Using this model, idealized measurements are described as certain averages of μ. In mathematical terms, the averages of μ define a linear transformation, called the *Radon transform*. These measurements are akin to the determination of the shadow function of a convex region described in Section 1.2. In Chapter 6 we show that if the Radon transform of μ could be measured exactly, then μ could be completely determined from this data. In reality, the data collected are a limited part of the mathematically "necessary" data, and the measurements are subject to a variety of errors. In later chapters we refine the measurement model and reconstruction algorithm to reflect more realistic models of the physical properties of x-rays and the data that are actually collected.

This chapter begins with a model for the interaction of x-rays with matter. To explicate the model we then apply it to describe several simple physical situations. After a short excursion into the realm of x-ray physics, we give a formal definition of the Radon transform and consider some of its simpler properties. The last part of the chapter is more mathematical, covering the inversion of the Radon transform on radial functions, the Abel transform, and a discussion of Volterra integral equations.

3.1 Tomography

Literally, tomography means *slice imaging*. Today this term is applied to many methods used to reconstruct the internal structure of a solid object from external measurements. In x-ray tomography the literal meaning persists in that we reconstruct a three-dimensional object from its two-dimensional slices. Objects of interest in x-ray imaging are described by a real-valued function defined on $\mathbb{R}^3$, called the *attenuation coefficient*. The attenuation coefficient quantifies the tendency of an object to absorb or scatter x-rays of a given energy. This function varies from point-to-point within the object and is usually taken to vanish

From "Introduction to the Mathematics of Medical Imaging, Second Edition" by Charles L. Epstein

Copyright ©2007 by the Society for Industrial and Applied Mathematics
This electronic version is for personal use and may not be duplicated or distributed.

Material	Attenuation coefficient in Hounsfield units
water	0
air	−1000
bone	1086
blood	53
fat	−61
brain white/gray	−4
breast tissue	9
muscle	41
soft tissue	51

Table 3.1. Attenuation coefficients of human tissues for 100-keV x-rays, adapted from [67].

outside it. The attenuation coefficient, like density, is nonnegative. It is useful for medical imaging because different anatomical structures have different attenuation coefficients. Bone has a much higher attenuation coefficient than soft tissue and different soft tissues have slightly different coefficients. For medical applications it is crucial that normal and cancerous tissues also have slightly different attenuation coefficients.

While in this book we work almost exclusively with the attenuation coefficient, as described previously, it is rarely used by radiologists. Instead the attenuation coefficient is compared to the attenuation coefficient water and quoted in terms of a dimensionless quantity called a *Hounsfield unit*. The normalized attenuation coefficient, in Hounsfield units is defined by

$$H_{\text{tissue}} = \frac{\mu_{\text{tissue}} - \mu_{\text{water}}}{\mu_{\text{water}}} \times 1000.$$

Unlike the actual attenuation coefficient, this relative measure assumes both positive and negative values. Table 3.1 lists typical normalized attenuation coefficients for different parts of the body.

The attenuation coefficients of air (−1000) and bone (1100) define the range of values present in a typical clinical situation. This means that the *dynamic range* of a clinical CT measurement is about 2000 Hounsfield units. From the table it is apparent that the variation in the attenuation coefficients of soft tissues is about 2% of this range. For x-ray CT to be clinically useful this means that the reconstruction of the attenuation coefficient must be accurate to about 10 Hounsfield units or less than a half a percent of its dynamic range.

Let μ be a function defined on $\mathbb{R}^3$. To define the slices of μ we need to fix a coordinate system $\boldsymbol{x} = (x_1, x_2, x_3)$. For each fixed value c of x_3, the x_3-slice of μ is the function of two variables, f_c, defined by

$$f_c(x_1, x_2) = \mu(x_1, x_2, c).$$

From "Introduction to the Mathematics of Medical Imaging, Second Edition" by Charles L. Epstein

Copyright ©2007 by the Society for Industrial and Applied Mathematics
This electronic version is for personal use and may not be duplicated or distributed.

A knowledge of the collection of functions $\{f_c : c \in [a, b]\}$ is equivalent to a knowledge of μ for all points in the slab

$$\{(x_1, x_2, x_3) : -\infty < x_1 < \infty, -\infty < x_2 < \infty, a \le x_3 \le b\}.$$

While the choice of coordinates is arbitrary, having a fixed frame of reference is a crucial element of any tomographic method. By convention the slices are defined by fixing the last coordinate. In general, different coordinate systems lead to different collections of slices. In actual practice the x-ray CT machine fixes the frame of reference.

***Definition* 3.1.1.** Let D be a subset of $\mathbb{R}^n$. The *characteristic function* of D is defined by

$$\chi_D(\boldsymbol{x}) = \begin{cases} 1 & \text{if } \boldsymbol{x} \in D, \\ 0 & \text{if } \boldsymbol{x} \notin D. \end{cases}$$

***Remark* 3.1.1.** Evaluation of χ_D at $\boldsymbol{x}$ is a simple mathematical model for an experiment that tries to decide whether or not the point $\boldsymbol{x}$ lies in the set D.

***Example* 3.1.1.** Let D be a subset of $\mathbb{R}^3$; the function χ_D models an object with constant attenuation coefficient. In this case the object is determined by its intersection with the planes

$$H_c = \{(x_1, x_2, c) : x_1, x_2 \in \mathbb{R}\}.$$

For each c we let $D_c = D \cap H_c$. Figure 3.1 shows a two-dimensional slice of a three-dimensional object.

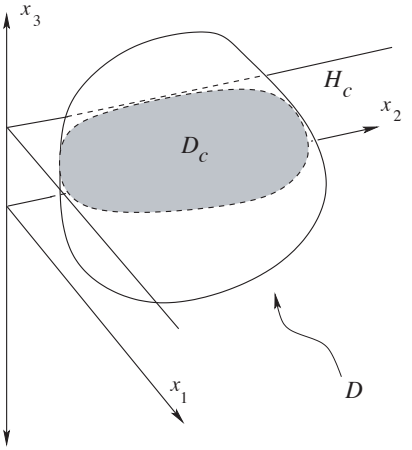

Figure 3.1. A 2D slice of a 3D object.

***Example* 3.1.2.** Suppose that the object is contained in the ball of radius 1 and its attenuation coefficient is

$$\mu(\boldsymbol{x}) = \begin{cases} 1 - \|\boldsymbol{x}\| & \text{if } \|\boldsymbol{x}\| \le 1, \\ 0 & \text{if } \|\boldsymbol{x}\| > 1. \end{cases}$$

From "Introduction to the Mathematics of Medical Imaging, Second Edition" by Charles L. Epstein

Copyright ©2007 by the Society for Industrial and Applied Mathematics
This electronic version is for personal use and may not be duplicated or distributed.

The slices of μ are the functions

$$f_c(x_1, x_2) = \begin{cases} 1 - \sqrt{x_1^2 + x_2^2 + c^2} & \text{if } \sqrt{x_1^2 + x_2^2 + c^2} \leq 1, \\ 0 & \text{if } \sqrt{x_1^2 + x_2^2 + c^2} > 1. \end{cases}$$

Note in particular that if $|c| > 1$, then $f_c \equiv 0$.

As these examples show, an important feature of a function is the set of points where it is nonzero. From the point of view of measurement it is difficult to distinguish points where a function is nonzero from points that are "arbitrarily close" to such points. Indeed, to get a useful mathematical concept we need to add points that are "arbitrarily close" to points where the function is nonzero. As the definition is the same in all dimensions we give it for functions defined on $\mathbb{R}^n$.

***Definition* 3.1.2.** Let f be a function defined on $\mathbb{R}^n$. A point $\boldsymbol{x}$ belongs to the *support* of f if there is a sequence of points $< \boldsymbol{x}_n >$ such that

1. $f(\boldsymbol{x}_n) \neq 0$,
2. $\lim_{n\to\infty} \boldsymbol{x}_n = \boldsymbol{x}$.

This set is denoted by $\text{supp}(f)$.

***Example* 3.1.3.** The support of the function $f(x) = x$ is the whole real line, even though $f(0) = 0$. The support of the function $f(x, y) = xy$ is the whole plane, even though $f(0, y) = f(x, 0) = 0$. The support of the function $\chi_{(0,1)}(x)$ is $[0, 1]$.

***Example* 3.1.4.** If D is a subset of $\mathbb{R}^n$ then the support of χ_D is the *closure* of D. This is the collection of all points which are limits of sequences contained in D. A set that contains all such limit points is called a *closed set*.

***Definition* 3.1.3.** A function f defined in $\mathbb{R}^n$ is said to have *bounded support* if there is an R so that $f(\boldsymbol{x}) = 0$ if $\|\boldsymbol{x}\| > R$. In this case we say that the support of f is contained in the ball of radius R.

For the purposes of medical imaging, air is usually assumed to be transparent to x-rays. This means that the attenuation coefficient is set to zero at points outside of the patient. The support of μ can therefore be determined by non-invasive measurements.

3.1.1 Beer's Law and X-ray Tomography

We now turn our attention to a simple quantitative model for the interaction of x-rays with matter. Sometimes x-rays are thought of as a flux of very high-energy, electromagnetic radiation. The x-ray beam is described by a vector valued function $\boldsymbol{I}(\boldsymbol{x})$. The direction of $\boldsymbol{I}$ at $\boldsymbol{x}$ is the direction of the flux at $\boldsymbol{x}$ and its magnitude,

$$I(\boldsymbol{x}) = \|\boldsymbol{I}(\boldsymbol{x})\|$$

is the intensity of the beam. If dS is an infinitesimal surface element at $\boldsymbol{x}$ of area $|dS|$, placed at right angles to $\boldsymbol{I}(\boldsymbol{x})$, then the energy-per-unit-time passing through dS is $I(\boldsymbol{x})|dS|$.

From "Introduction to the Mathematics of Medical Imaging, Second Edition" by Charles L. Epstein

Copyright ©2007 by the Society for Industrial and Applied Mathematics
This electronic version is for personal use and may not be duplicated or distributed.

More generally, the intensity of the beam passing through the infinitesimal area element dS, located at $\boldsymbol{x}$, with unit normal vector $\boldsymbol{n}(\boldsymbol{x})$, is

$$\langle \boldsymbol{I}(\boldsymbol{x}), \boldsymbol{n}(\boldsymbol{x}) \rangle \, |dS|.$$

The total intensity passing through a surface S is the surface integral

$$\int_S \langle \boldsymbol{I}(\boldsymbol{x}), \boldsymbol{n}(\boldsymbol{x}) \rangle \, dA_S,$$

where dA_S is the area element on S.

In other circumstances it is more useful to describe an x-ray beam as being composed of a stream of discrete particles called *photons*. Each photon has a well defined energy, often quoted in units of *electron-volts*. The energy E is related to electromagnetic frequency ν by de Broglie's Law:

$$E = h\nu;$$

h is Planck's constant. While the photon description is more correct, quantum mechanically, the two descriptions only differ significantly when the number of photons (or the intensity of the beam) is small.

Our model for the interaction of x-rays with matter is phrased in terms of the continuum model; it rests on three basic assumptions:

(1) NO REFRACTION OR DIFFRACTION: X-ray beams travel along straight lines that are not "bent" by the objects they pass through.

(2) THE X-RAYS USED ARE MONOCHROMATIC: The waves making up the x-ray beam are all of the same frequency.

(3) BEER'S LAW: Each material encountered has a characteristic linear attenuation coefficient μ for x-rays of a given energy. The intensity, I of the x-ray beam satisfies Beer's law

$$\frac{dI}{ds} = -\mu(\boldsymbol{x})I. \tag{3.1}$$

Here s is the arc-length along the straight-line trajectory of the x-ray beam.

Because x-rays have very high energies, and therefore very short wavelengths, assumption (1) is a good approximation to the truth. Ordinary light is also electromagnetic radiation, we experience the frequency of this radiation as the color of the light. The second assumption is that the x-ray beam is "all of one color." This is not a realistic assumption, but it is needed to construct a *linear* model for the measurements. The implications of the failure of this assumption are discussed later in this chapter. If we think of the x-ray beam as a stream of photons, then the beam is monochromatic if all the photons in the beam have the same energy E. The intensity $I(\boldsymbol{x})$ then equals $EN(\boldsymbol{x})$. Here $N(\boldsymbol{x})$ is the *photon flux*, or the number of photons per unit time crossing a surface at right angles to $\boldsymbol{I}(\boldsymbol{x})$. If the beam is not monochromatic, then the relationship between the intensity and photon flux is described by the spectral function which is introduced in Section 3.3.

From "Introduction to the Mathematics of Medical Imaging, Second Edition" by Charles L. Epstein

Copyright ©2007 by the Society for Industrial and Applied Mathematics
This electronic version is for personal use and may not be duplicated or distributed.

Beer's law requires some explanation. Suppose that an x-ray beam encounters an object. Beer's law describes how the presence of the object affects the intensity of the beam. For the moment suppose that we live in a one-dimensional world, with s a coordinate in our world. Let $I(s)$ be the intensity of the x-ray beam at s. For a one-dimensional problem I would be quoted in units of electron-volts/s. Beer's law predicts the change in intensity due to the material lying between s and $s + \Delta s$:

$$I(s + \Delta s) - I(s) \approx -\mu(s) I(s)\, \Delta s. \tag{3.2}$$

Think now of the beam as being composed of a large number, $N(s)$ photons/second, each of the given energy E traveling along the same straight line. Then $I(s) = EN(s)$ and equation (3.2) implies that

$$N(s + \Delta s) - N(s) \approx -\mu(s) N(s)\, \Delta s.$$

This formulation suggests a probabilistic interpretation for Beer's law: $\mu(s)\Delta s$ can be regarded as giving the probability that a photon incident on the material at coordinate s is absorbed. We return to this in Section 16.1.2.

Using the assumption that x-rays travel along straight lines, Beer's law is easily applied to two- and three-dimensional problems. The two- or three-dimensional x-ray flux is modeled as a collection of noninteracting, one-dimensional beams. As noted previously, the x-ray flux at a point $\boldsymbol{x}$ is described by a vector $\boldsymbol{I}(\boldsymbol{x})$. In light of assumption (1) the direction of $\boldsymbol{I}$ at $\boldsymbol{x}$ gives the direction of the *straight line* along which the beam is traveling. Suppose that one of the x-ray beams is traveling along the line given parametrically by

$$\{\boldsymbol{x}_0 + s\boldsymbol{v} \ : \ s \in \mathbb{R}\}.$$

Here $\boldsymbol{v}$ is a unit vector in $\mathbb{R}^3$. The function

$$i(s) = I(\boldsymbol{x}_0 + s\boldsymbol{v})$$

gives the intensity of the beam at points along this line, and

$$m(s) = \mu(\boldsymbol{x}_0 + s\boldsymbol{v})$$

gives the attenuation coefficient. Beer's law states that

$$\frac{di}{ds} = -m(s) i(s) \text{ or } \frac{d(\log i)}{ds} = -m(s).$$

Integrating this equation from $s = a$ to $s = b$ gives

$$\log\left[\frac{i(b)}{i(a)}\right] = -\int_a^b m(s)\, ds.$$

From "Introduction to the Mathematics of Medical Imaging, Second Edition" by Charles L. Epstein

Copyright ©2007 by the Society for Industrial and Applied Mathematics
This electronic version is for personal use and may not be duplicated or distributed.

Between the points $\boldsymbol{x}_0 + a\boldsymbol{v}$ and $\boldsymbol{x}_0 + b\boldsymbol{v}$, the intensity of the beam is attenuated by

$$\exp\left[-\int_a^b m(s)\,ds\right].$$

Typical units for the intensity of an x-ray beam are electron-volts/(s×cm^2) in three-dimensions and electron-volts/(s×cm) in two-dimensions. Beer's law describes how the material attenuates each of these one-dimensional beams; it implicitly asserts that the attenuation of x-rays is an isotropic process: It does not depend on the direction of the line along which the x-ray travels. An application of Beer's law to a two-dimensional situation is considered next.

***Example* 3.1.5.** Assume that we have a point source of x-rays of intensity I_0 in the plane [see Figure 3.2(a)]. The x-ray source is isotropic which means the outgoing flux is the same in all directions.

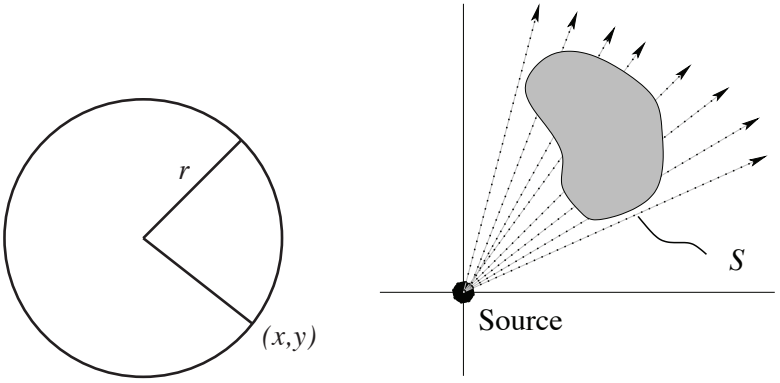

(a) A point source of x-rays

(b) The flux through a curve not enclosing the source is zero.

Figure 3.2. Analysis of an isotropic point source.

Because the source is isotropic, the intensity of the beam is only a function of the distance to the source. Let $I(r)$ denote the intensity of the flux at distance r from the source. By conservation of energy,

$$I_0 = \int_{x^2+y^2=r^2} I(r)\,ds = 2\pi r I(r). \tag{3.3}$$

The intensity of the beam at distance r from the source is therefore

$$I(r) = \frac{I_0}{2\pi r}. \tag{3.4}$$

The x-ray flux is modeled as beams traveling along the rays that pass through the source. If I_0 is measured in units of electron-volts/second, then $I(r)$ has units $\frac{\text{electron-volts}}{\text{cm}\times\text{second}}$.

From "Introduction to the Mathematics of Medical Imaging, Second Edition" by Charles L. Epstein

Copyright ©2007 by the Society for Industrial and Applied Mathematics
This electronic version is for personal use and may not be duplicated or distributed.

Fixing coordinates so that the source is placed at $(0, 0)$, the x-ray flux at a point (x, y) travels along the line from (x, y) to $(0, 0)$ and is given by

$$\begin{aligned} \boldsymbol{I}(x, y) = I(r)\frac{(x, y)}{\sqrt{x^2 + y^2}} = I_0\frac{\hat{r}}{2\pi r}, \\ \text{where } \hat{r} = \frac{(x, y)}{r}, \quad r = \sqrt{x^2 + y^2}. \end{aligned} \tag{3.5}$$

If a curve S does not enclose the source, then conservation of energy implies that

$$\int_S \boldsymbol{I}(x, y)\hat{r} \cdot \hat{n}\, ds = 0; \tag{3.6}$$

here $\hat{n}$ is the outward normal vector to S. As the curve encloses no sources or sinks, the line integral of the flux is zero: everything that comes into this surface has to go out.

For a point source the intensity of the rays diminish as you move away from the source; this is called beam spreading. Beer's law can be used to model this effect. Let μ_s denote the attenuation coefficient that accounts for the spreading of the beam. As a guess we let $\mu_s = 1/r$ and see that

$$\frac{dI}{dr} = -\frac{1}{r}I \Rightarrow \frac{d\log I}{dr} = -\frac{1}{r}. \tag{3.7}$$

Integrating equation (3.7) from an $r_0 > 0$ to r gives

$$I(r) = I(r_0)\frac{r_0}{r}.$$

This agrees with (3.4). That we cannot integrate down to $r = 0$ reflects the non-physical nature of a point source. In x-ray tomography it is often assumed that the attenuation of the beam due to beam spreading is sufficiently small, compared to the attenuation due to the object that it can be ignored. This is called a *non-diverging source* of x-rays.

In a real measurement, the x-ray source is turned on for a known period of time. The total energy, I_i, incident on the object along a given line, l is known. The total energy, I_o, emerging from the object along l is then measured by an x-ray detector. Integrating Beer's law we obtain

$$\log\frac{I_o}{I_i} = -\int_l \mu\, ds. \tag{3.8}$$

Here ds is the arc length parameter along the straight line path l. A perfect measurement of the ratio I_o/I_i would therefore furnish the line integral of the attenuation coefficient along the line l. Indeed we model the measurements made in x-ray tomography as precisely these line integrals.

An ordinary x-ray image is formed by sending a beam of x-rays through an object, with the detector a sheet of photographic film. Suppose that the x-rays travel along parallel lines, passing through an object before arriving on a photographic plate, as shown in Figure 3.3. By measuring the density of the exposed film, we can determine the intensity of the x-ray

From "Introduction to the Mathematics of Medical Imaging, Second Edition" by Charles L. Epstein

Copyright ©2007 by the Society for Industrial and Applied Mathematics
This electronic version is for personal use and may not be duplicated or distributed.

beam at the surface of the film. More absorbent parts of an object result in fewer x-rays photons at the surface of the film. If the intensity of the incident beam is known, then the density of the film can be used to determine the integrals of the attenuation coefficient along this family of parallel lines.

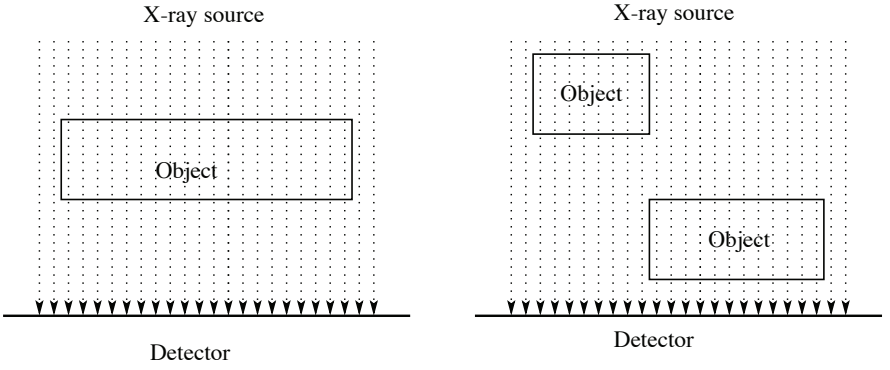

(a) One object. (b) Two objects.

Figure 3.3. The failure of ordinary x-ray images to distinguish objects.

The result is a "projection" or shadow of the object. The shadows of the objects in Figures 3.3(a) and (b) are the same, so it is not possible to distinguish between them using this projection. Placing the x-ray source at a different angle gives a different measurement. The measurement in Figure 3.4 distinguishes between the objects in Figures 3.3(a) and (b).

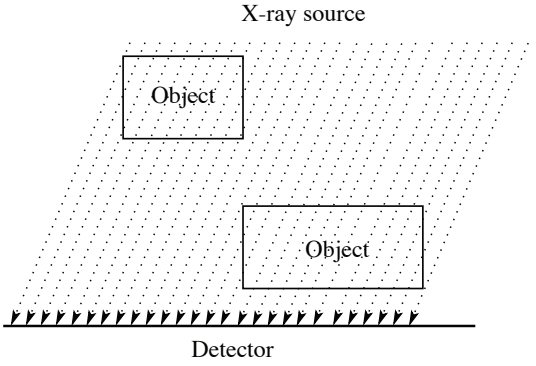

Figure 3.4. A different projection.

The principle is clear: The more directions from which you make measurements, the more arrangements of objects you can distinguish. The goal of x-ray tomography is much more ambitious; we would like to use these projections to reconstruct a picture of the slice. This problem is similar to that considered in Example 1.1.5. However, it is much more challenging to reconstruct a function from its averages along lines than to reconstruct the

From "Introduction to the Mathematics of Medical Imaging, Second Edition" by Charles L. Epstein

Copyright ©2007 by the Society for Industrial and Applied Mathematics
This electronic version is for personal use and may not be duplicated or distributed.

outline of an object from its shadows. To accomplish this in principle and in practice requires a great deal more mathematics.

Exercises

***Exercise* 3.1.1.** Suppose that we have an isotropic point source of x-rays in three-dimensions of intensity I_0. Find the formula for the intensity of the beams at a distance r from the source. What are the units of $I(r)$?

***Exercise* 3.1.2.** Verify (3.6) by direct computation.

***Exercise* 3.1.3.** Describe an apparatus that would produce a uniform, non-divergent source of x-rays.

3.2 Analysis of a Point Source Device

In this section we use Beer's law to study a simple two-dimensional apparatus and analyze what it measures. Figure 3.5 shows an apparatus with a point source of x-rays, an attenuating body and a photographic plate. We derive an expression for the flux at a point P on the photographic plate in terms of the attenuation of the beam caused by the object as well as beam spreading. The final expression involves the line integral of the attenuation coefficient.

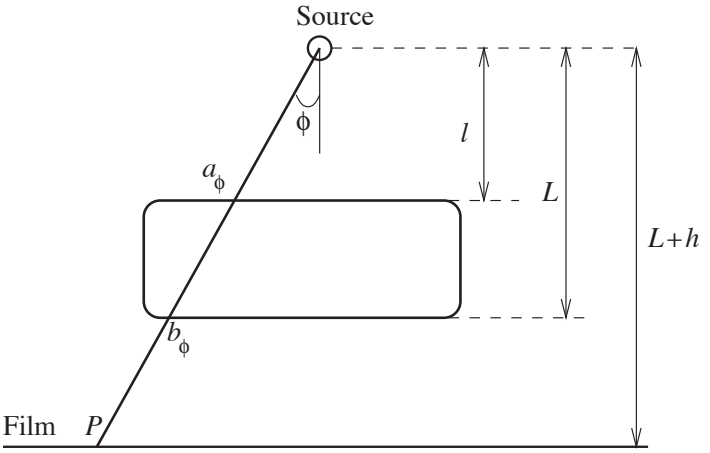

Figure 3.5. A point source device for measuring line integrals of the attenuation coefficient.

The geometry of our apparatus suggests the use of polar coordinates to label points in the plane. Let r denote the distance from the source and ϕ the angle indicated in the diagram. The attenuation coefficient for the absorbing body in Figure 3.5 is then a function of (r, ϕ), denoted by $\mu_a(r, \phi)$. The effect of beam spreading on the intensity of the flux is analyzed in Example 3.1.5. The total attenuation coefficient is obtained by adding $\mu_s(r) = r^{-1}$ to μ_a. For the beam of x-rays traveling along the line through the source, at angle ϕ,

From "Introduction to the Mathematics of Medical Imaging, Second Edition" by Charles L. Epstein

Copyright ©2007 by the Society for Industrial and Applied Mathematics
This electronic version is for personal use and may not be duplicated or distributed.

the differential equation describing the attenuation of the x-ray beam is

$$\frac{dI}{dr} = -\left(\mu_a(r,\phi) + \frac{1}{r}\right) I. \tag{3.9}$$

The sum, $\mu_a + r^{-1}$, is an *effective* attenuation coefficient as it captures both the attenuation due to the object and that due to beam spreading. The film is exposed by turning the source on for a known period of time. In order to avoid introducing more notation, I is also used to denote the total energy per unit length resulting from this exposure. The units for I in this case would be electron-volts/cm.

Label the radius of the first point of intersection of the line at angle ϕ with the absorbing body by a_ϕ, and the last by b_ϕ. The other distances describing the apparatus are labeled by h, L, and $L+h$, respectively. Integrating equation (3.9) from $r = r_0$ to the film plane $r = r_\phi$ gives

$$\log \frac{I(r_\phi,\phi)}{I(r_0,\phi)} = \log \frac{r_0}{r_\phi} - \int_{a_\phi}^{b_\phi} \mu_a(s,\phi)\, ds.$$

Using

$$a_\phi = \frac{l}{\cos\phi}, \quad b_\phi = \frac{L}{\cos\phi}, \quad r_\phi = \frac{L+h}{\cos\phi},$$

we get

$$I(r_\phi,\phi) = I_0 \frac{\cos\phi}{2\pi(L+h)} \exp\left[-\int_{a_\phi}^{b_\phi} \mu_a(s,\phi)\, ds\right].$$

The density of the developed film at a point is proportional to the logarithm of the total energy incident at that point; that is,

$$\text{density of the film} = \gamma \times \log(\text{total energy intensity,}) \tag{3.10}$$

where γ is a constant. We now compute this energy. As the film plane is not perpendicular to the direction of the beam of x-rays, we need to determine the flux across the part of the film subtended by the angle $\Delta\phi$. It is given by

$$\Delta F = \int_{\phi}^{\phi+\Delta\phi} I(r_\phi,\phi)\hat{r}\cdot\hat{n}\, d\sigma, \quad \hat{r} = -(\sin\phi, \cos\phi).$$

Here $\hat{n} = (0,-1)$ is the outward, unit normal vector to the film plane and $d\sigma$ is the arc length element along the film plane. In polar coordinates it is given by

$$d\sigma = \frac{L+h}{\cos^2\phi} d\phi.$$

From "Introduction to the Mathematics of Medical Imaging, Second Edition" by Charles L. Epstein

Copyright ©2007 by the Society for Industrial and Applied Mathematics
This electronic version is for personal use and may not be duplicated or distributed.

Since $\Delta\phi$ is small, we can approximate the integral by

$$\Delta F \approx \int_{\phi}^{\phi+\Delta\phi} I(r_\phi, \phi)\hat{r}\cdot\hat{n}\frac{L+h}{\cos^2\phi}d\phi \approx I_0\frac{\cos^2\phi}{2\pi(L+h)}\exp\left[-\int_{a_\phi}^{b_\phi}\mu_a(s,\phi)\,ds\right]\frac{L+h}{\cos^2\phi}\Delta\phi. \tag{3.11}$$

The length of film subtended by the angle $\Delta\phi$ is approximately

$$\Delta\sigma = \frac{L+h}{\cos^2\phi}\Delta\phi.$$

The energy density at the point P_ϕ, where the line making angle ϕ with the source, meets the film plane, is ΔF divided by this length. Indeed, letting $\Delta\phi$ tend to zero gives

$$\frac{dF}{d\sigma} = \frac{I_0\cos^2\phi}{2\pi(L+h)}\exp\left[-\int_{a_\phi}^{b_\phi}\mu_a(s,\phi)\,ds\right].$$

According to (3.10), the density of the film at P_ϕ is therefore

$$\gamma\,\log\frac{dF}{d\sigma} = \gamma\left[\log\frac{I_0\cos^2\phi}{2\pi(L+h)} - \int_{a_\phi}^{b_\phi}\mu_a(s,\phi)\,ds\right].$$

The first term comes from the attenuation due to beam spreading. Subtracting it from the measurement gives the line integral of the attenuation coefficient of the absorbing body along the ray at angle ϕ. Let $\delta(\phi)$ denote the density of the film at P_ϕ, this formula can be rewritten

$$-\int_{a_\phi}^{b_\phi}\mu_a(s,\phi)\,ds = \gamma^{-1}\delta(\phi) - \log\left[\frac{I_0\cos^2\phi}{2\pi(L+h)}\right].$$

On the right-hand side are quantities determined by measurement; the left-hand side is the line integral of the attenuation coefficient. This formula expresses the measurements as a *linear function* of the attenuation coefficient.

By varying the position of the source, we can measure the line integrals of the attenuation coefficient along another family of lines. If we move the source and film plane together, around a circle enclosing the absorbent material, making the measurements described previously for each position of the source, then we can measure the line integrals of the attenuation coefficient for all lines that intercept the object (Figure 3.6). This brings us to an essentially mathematical problem: Can a function be recovered from a knowledge of its line integrals along **all** lines? We shall see that this can in principle be done. That it can also be done in practice forms the basis for image reconstruction in an x-ray CT machine.

From "Introduction to the Mathematics of Medical Imaging, Second Edition" by Charles L. Epstein

Copyright ©2007 by the Society for Industrial and Applied Mathematics
This electronic version is for personal use and may not be duplicated or distributed.

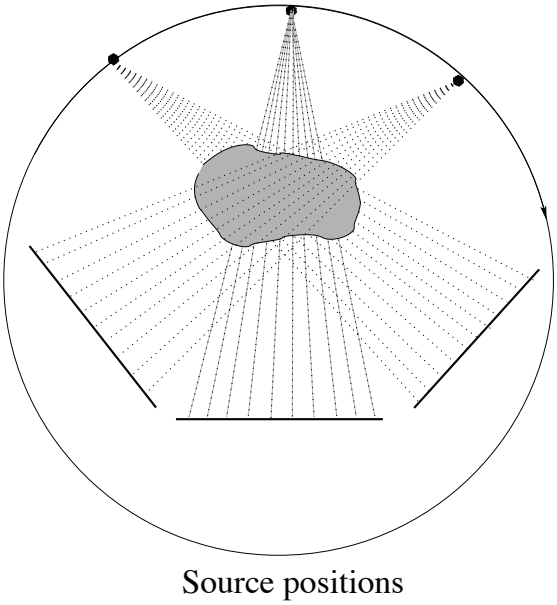

Figure 3.6. Collecting data from many views.

We now describe a idealized model for what is measured in x-ray tomography. As remarked above the CT machine determines a coordinate system (x_1, x_2, x_3) for $\mathbb{R}^3$. Let μ denote the attenuation coefficient of an object. Suppose the support of μ lies in the cube $[-a, a] \times [-a, a] \times [-a, a]$. For each c between $\pm a$ and each pair $(t, \boldsymbol{\omega}) \in \mathbb{R} \times S^1$ we measure integral of μ along the line

$$\{(x_1, x_2, x_3) : \ x_3 = c \text{ and } \langle (x_1, x_2), \boldsymbol{\omega} \rangle = t\},$$

that is,

$$\int_{-\infty}^{\infty} \mu(t\boldsymbol{\omega} + s\hat{\boldsymbol{\omega}}, c)\, ds.$$

We measure the line integrals of μ along all lines that lie in planes where x_3 is constant.

Figure 3.7(a) is a density plot of a function that models the attenuation coefficient of a slice of the human head. The densities in this plot are scaled so that the highest attenuation (the skull) is white and the lowest (surrounding air) is black. A model of this sort is called a *mathematical phantom*. Such models were introduced into medical image reconstruction by Larry Shepp. These are discussed in greater detail in Section 11.2. The example shown in Figure 3.7(a) is adapted from a paper by Shepp and Logan, [114]. Figure 3.7(b) depicts the line integrals of this function. The horizontal axis is the angular variable, with θ corresponding to $\boldsymbol{\omega}(\theta) = (\cos(\theta), \sin(\theta))$. The angle varies between 0 and 2π. The vertical axis is the affine parameter. Again white corresponds to high densities and black to low densities.

From "Introduction to the Mathematics of Medical Imaging, Second Edition" by Charles L. Epstein

Copyright ©2007 by the Society for Industrial and Applied Mathematics
This electronic version is for personal use and may not be duplicated or distributed.

(a) A density plot of the Shepp-Logan phantom.

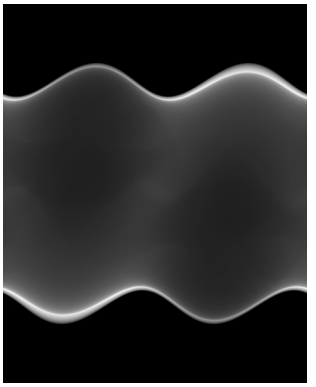

(b) The line integrals for the function shown in (a).

Figure 3.7. The line integrals of the Shepp-Logan phantom.

In Chapter 6 we give a formula for determining a function defined in $\mathbb{R}^2$ from its integrals on *all* lines in the plane. Of course, it is not possible to make an infinite number of measurements. This means that we need a method for reconstructing an approximation to a function from a finite collection of line integrals. In Chapter 11, beginning with the exact reconstruction formula, we obtain algorithms for use with finitely many measurements.

Exercises

***Exercise* 3.2.1.** Explain why the top and bottom of Figure 3.7(b) are identical.

***Exercise* 3.2.2.** Why is Figure 3.7(b) black near the left and right edges?

***Exercise* 3.2.3.** Explain the significance of the white bands in Figure 3.7(b).

3.3 Some Physical Considerations

Before proceeding with the mathematical development, we briefly revisit the assumptions underlying our model for the attenuation of x-rays. This discussion previews topics considered in later chapters and is not essential to the remainder of this chapter. The x-ray source is assumed to be monochromatic. In fact, the beam of x-rays is made up of photons having a wide range of energies. The distribution of photon energies is described by its *spectral function*, S. If $\mathscr{E}_1$ and $\mathscr{E}_2$ are nearby energies, then the energy in the beam due to photons with energies lying in the interval $[\mathscr{E}_1, \mathscr{E}_2]$ is about $S(\mathscr{E}_1)(\mathscr{E}_2 - \mathscr{E}_1)$, or more precisely

$$\int_{\mathscr{E}_1}^{\mathscr{E}_2} S(\mathscr{E})\, d\mathscr{E}.$$

From "Introduction to the Mathematics of Medical Imaging, Second Edition" by Charles L. Epstein

Copyright ©2007 by the Society for Industrial and Applied Mathematics
This electronic version is for personal use and may not be duplicated or distributed.

The graph of a typical spectral function is shown in Figure 3.8. The total energy output of the source is given by

$$\Psi_i = \int_0^\infty S(\mathscr{E})d\mathscr{E}.$$

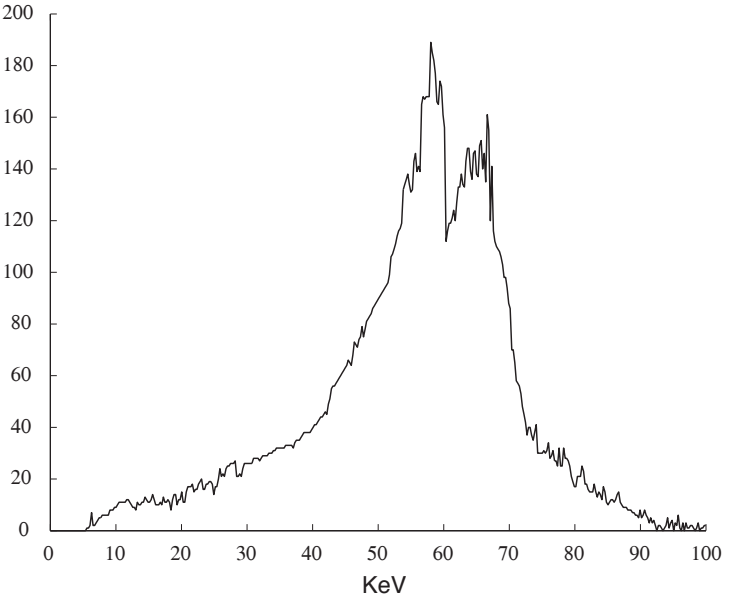

Figure 3.8. A typical x-ray source spectral function. (Spectral data provided by Dr. Andrew Karellas, University of Massachusetts Medical School, Department of Radiology, Worcester, Massachusetts.)

The attenuation coefficient of a given material is a complicated function of the energy, monotonely decreasing as the energy increases. The attenuation coefficient is the sum total of the results of several physical processes that x-rays undergo. A discussion of the physics behind the attenuation coefficient can be found in [6]. Let $\mu(\boldsymbol{x}, \mathscr{E})$ denote the attenuation coefficient of the object at $\boldsymbol{x}$ for photons of energy $\mathscr{E}$. Beer's law, applied to the photons of energy $\mathscr{E}$, traveling along a line l states that the ratio $I_o(\mathscr{E})/I_i(\mathscr{E})$ of emitted flux to incident flux at this energy is

$$\frac{I_o(\mathscr{E})}{I_i(\mathscr{E})} = \exp\left[-\int_l \mu(\boldsymbol{x}, \mathscr{E})\, ds\right].$$

The incident flux at energy $\mathscr{E}$ is $S(\mathscr{E})\, d\mathscr{E}$ and therefore

$$I_o(\mathscr{E}) = S(\mathscr{E})\, d\mathscr{E} \exp\left[-\int_l \mu(\boldsymbol{x}, \mathscr{E})\, ds\right].$$

From "Introduction to the Mathematics of Medical Imaging, Second Edition" by Charles L. Epstein

Copyright ©2007 by the Society for Industrial and Applied Mathematics
This electronic version is for personal use and may not be duplicated or distributed.

Because low-energy (or soft) x-rays are attenuated more efficiently than high-energy (or hard) x-rays, the distribution of energies in the output beam is skewed toward higher energies. In medical imaging, this is called *beam hardening*. Along a given line the spectral function at energy $\mathscr{E}$ of the output beam is

$$S_{\text{out}}(\mathscr{E}) = S(\mathscr{E}) \exp\left[-\int_l \mu(x, \mathscr{E}) ds \right].$$

Integrating S_{out} over the energy gives the measured output

$$\Psi_o = \int_0^\infty S(\mathscr{E}) \exp\left[-\int_l \mu(\boldsymbol{x}, \mathscr{E})\, ds \right] d\mathscr{E}.$$

As before, we would like to reconstruct μ or perhaps some average of this function over energies. Mathematically this is a *very* difficult problem as the measurement, Ψ_o, is a non-linear function of μ. We have avoided this problem by assuming that the x-ray beam used to make the measurements is monochromatic. This provides the much simpler *linear* relationship (3.8) between the measurements and the attenuation coefficient. In Chapter 12 we briefly consider the artifacts that result from using polychromatic x-rays and methods used to ameliorate them.

The fact that the x-ray "beam" is not a continuous flux but is composed of discrete particles produces random errors in the measurements. This type of error is called Poisson noise, quantum noise, or photon noise. In Chapter 16 we analyze this effect, showing that the available information in the data is proportional to the square root of the *number* of photons used to make the measurement. The accuracy of the measurements is the ultimate limitation on the number of significant digits in the reconstructed attenuation coefficient. Table 3.1 lists the attenuation coefficients of different structures encountered in medical CT. The attenuation coefficients of air (-1000) and bone (1086) define the range of values present in a typical clinical situation. The dynamic range of a clinical CT measurement is about 2000 Hounsfield units. From the table it is apparent that the variation in the attenuation coefficients of soft tissues is about 2% of this range. For x-ray CT to be clinically useful this means that the reconstruction of the attenuation coefficient needs to be accurate to less than a half a percent.

An obvious solution to this problem would be to increase the number of photons. Since each x-ray photon carries a very large amount of energy, considerations of patient safety preclude this solution. The number of x-ray photons involved in forming a CT image is approximately $10^7/\,\text{cm}^2$. This should be compared with the 10^{11} to $10^{12}/\,\text{cm}^2$ photons, needed to make a usable photographic image. In ordinary photography, quantum noise is not a serious problem because the number of photons involved is very large. In x-ray tomography, patient safety and quantum noise place definite limits on the contrast and resolution of a CT image.

From "Introduction to the Mathematics of Medical Imaging, Second Edition" by Charles L. Epstein

Copyright ©2007 by the Society for Industrial and Applied Mathematics
This electronic version is for personal use and may not be duplicated or distributed.

3.4 The Definition of the Radon Transform

See: A.3, A.4.1.

The first step in determining a function from its integrals along all straight lines is to organize this information in a usable fashion. We use the parameterization for the set of oriented lines in the plane described in Section 1.2.1. Recall that for $(t, \boldsymbol{\omega}) \in \mathbb{R} \times S^1$, $l_{t,\boldsymbol{\omega}}$ is the set

$$\{\boldsymbol{x} \in \mathbb{R}^2 \mid \langle \boldsymbol{x}, \boldsymbol{\omega} \rangle = t\},$$

with orientation determined by $\hat{\boldsymbol{\omega}}$ (Figure 1.12).

***Definition* 3.4.1.** Suppose that f is a function defined in the plane, which, for simplicity, we assume is continuous with bounded support. The integral of f along the line $l_{t,\boldsymbol{\omega}}$ is denoted by

$$\begin{aligned} \mathcal{R}f(t, \boldsymbol{\omega}) &= \int_{l_{t,\boldsymbol{\omega}}} f\, ds \\ &= \int_{-\infty}^{\infty} f(s\hat{\boldsymbol{\omega}} + t\boldsymbol{\omega}) ds \\ &= \int_{-\infty}^{\infty} f(t\omega_1 - s\omega_2, t\omega_2 + s\omega_1)\, ds. \end{aligned} \tag{3.12}$$

The collection of integrals of f along the lines in the plane defines a function on $\mathbb{R} \times S^1$, called the *Radon transform* of f.

***Example* 3.4.1.** In this example we give a graphical description for the computation of the Radon transform. Figure 3.9(a) shows the graph of a function f defined in the plane along with some lines in the family

$$\{\langle \boldsymbol{x}, (\cos(\frac{\pi}{4}), \sin(\frac{\pi}{4}))\rangle = t\}.$$

In Figure 3.9(b) we show graphs of f restricted to these lines. Behind the slices is the graph of $\mathcal{R}f(t, (\cos(\frac{\pi}{4}), \sin(\frac{\pi}{4})))$. The height of this curve at each point is just the area under the corresponding slice of the graph of f.

From "Introduction to the Mathematics of Medical Imaging, Second Edition" by Charles L. Epstein

Copyright ©2007 by the Society for Industrial and Applied Mathematics
This electronic version is for personal use and may not be duplicated or distributed.

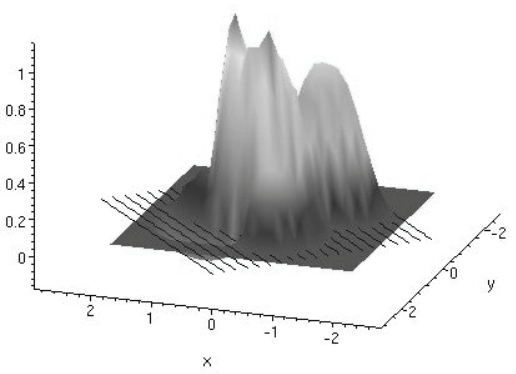

(a) The graph of f and a family of parallel lines in the plane.

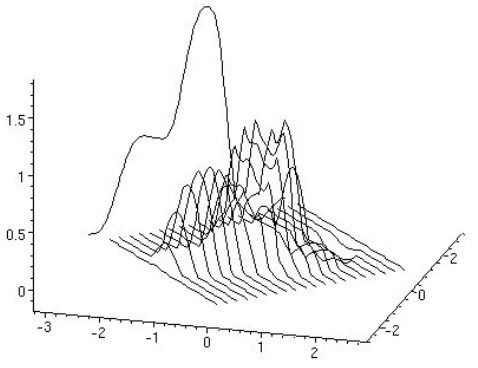

(b) Slices of f and its Radon transform for this family of lines.

Figure 3.9. Graphical depiction of the Radon transform.

It is not necessary for f to be either continuous or of bounded support. The Radon transform can be defined, a priori for a function, f whose restriction to each line is *locally integrable* and

$$\int_{-\infty}^{\infty} |f(t\boldsymbol{\omega} + s\hat{\boldsymbol{\omega}})\, ds| < \infty \text{ for all } (t, \boldsymbol{\omega}) \in \mathbb{R} \times S^1. \tag{3.13}$$

With these conditions the improper integrals in (3.12) are unambiguously defined. Functions that satisfy (3.13) are in the *natural domain* of the Radon transform. This is really two different conditions:

1. The function is regular enough so that restricting it to any line gives a locally integrable function.

2. The function goes to zero rapidly enough for the improper integrals to converge.

The function $f \equiv 1$ is not in the natural domain of the Radon transform because it does not decay at infinity. The function $f(x, y) = (x^2 + y^2)^{-1}$ is not in the natural domain of $\mathcal{R}$ because the integrals in (3.13) diverge if $t = 0$. While an understanding of the domain of Radon transform is a important part of its mathematical analysis. In applications to medical imaging, functions of interest are usually piecewise continuous and zero outside of some disk and therefore belong to the natural domain of $\mathcal{R}$.

Functions in the range of the Radon transform have a special symmetry property.

***Definition* 3.4.2.** A function h on $\mathbb{R} \times S^1$ is an *even function* if

$$h(t, \boldsymbol{\omega}) = h(-t, -\boldsymbol{\omega}). \tag{3.14}$$

We summarize the elementary properties of the Radon transform in a proposition.

From "Introduction to the Mathematics of Medical Imaging, Second Edition" by Charles L. Epstein

Copyright ©2007 by the Society for Industrial and Applied Mathematics
This electronic version is for personal use and may not be duplicated or distributed.

Proposition 3.4.1. *The Radon transform is linear; that is, if f and g are functions in the natural domain of the Radon transform, then*

$$\begin{aligned} \mathcal{R}(af) &= a\,\mathcal{R}f \text{ for all } a \in \mathbb{R} \text{ and} \\ \mathcal{R}(f+g) &= \mathcal{R}f + \mathcal{R}g. \end{aligned} \tag{3.15}$$

The Radon transform of f is an even function; that is,

$$\mathcal{R}f(t,\boldsymbol{\omega}) = \mathcal{R}f(-t,-\boldsymbol{\omega}). \tag{3.16}$$

The Radon transform is monotone: if f is a non-negative function in the natural domain of the Radon transform then

$$\mathcal{R}f(t,\boldsymbol{\omega}) \geq 0 \quad \textit{for every } (t,\boldsymbol{\omega}). \tag{3.17}$$

Proof. The linearity is a consequence of the linearity of integration over a line. The second statement follows from the fact that, as sets, $l_{t,\boldsymbol{\omega}} = l_{-t,-\boldsymbol{\omega}}$. The last statement follows from the analogous property for the integral. □

We now define some simple classes of functions and compute their Radon transforms.

***Example* 3.4.2.** Let E be a subset of $\mathbb{R}^2$; the Radon transform of χ_E has a simple geometric description.

$$\mathcal{R}\chi_E(t,\boldsymbol{\omega}) = \text{ the length of the intersection } l_{t,\boldsymbol{\omega}} \cap E.$$

If E is a closed, bounded subset, then χ_E belongs to the natural domain of the Radon transform. These functions model objects with constant attenuation coefficient.

In some cases it is possible to give a more explicit formula for $\mathcal{R}\chi_E$.

***Definition* 3.4.3.** The ball in $\mathbb{R}^n$ of radius r centered at $\boldsymbol{a}$ is denoted

$$B_r(\boldsymbol{a}) = \{\boldsymbol{x} \,:\, \|\boldsymbol{x}-\boldsymbol{a}\| < r\}.$$

Often $B_r(\mathbf{0})$ is denoted by B_r. Balls in $\mathbb{R}^2$ are often called *disks*.

***Example* 3.4.3.** Consider the disk of radius 1 in $\mathbb{R}^2$. The function χ_{B_1} is a special case of the general class considered in the previous example. The formula for the Radon transform of χ_{B_1} is

$$\mathcal{R}\chi_{B_1}(t,\boldsymbol{\omega}) = \begin{cases} 2\sqrt{1-t^2} & \text{if } |t| \leq 1, \\ 0 & \text{if } |t| > 1. \end{cases}$$

Note that $|t| > 1$ corresponds to lines $l_{t,\boldsymbol{\omega}}$ that do not intersect B_1.

***Definition* 3.4.4.** A function, f defined on $\mathbb{R}^n$ is *radial* if its value only depends on the distance to the origin. In this case there exists a function, F, of a single variable so that

$$f(\boldsymbol{x}) = F(\|\boldsymbol{x}\|).$$

Copyright ©2007 by the Society for Industrial and Applied Mathematics
This electronic version is for personal use and may not be duplicated or distributed.

***Example* 3.4.4.** The Radon transform of a radial function takes a simpler form. From geometric considerations it is clear that $\mathcal{R}f(t, \boldsymbol{\omega})$ does not depend on $\boldsymbol{\omega}$. Fixing a convenient direction—for example, $\boldsymbol{\omega} = (1, 0)$—we obtain

$$\begin{aligned} \mathcal{R}f(t, \boldsymbol{\omega}) &= \int_{-\infty}^{\infty} f(t, s)\, ds \\ &= \int_{-\infty}^{\infty} F(\sqrt{t^2 + s^2})\, ds. \end{aligned} \tag{3.18}$$

Using the change of variable, $r^2 = t^2 + s^2$, $2r\, dr = 2s\, ds$, we obtain

$$\mathcal{R}f(t, \boldsymbol{\omega}) = 2 \int_{t}^{\infty} \frac{F(r) r\, dr}{\sqrt{r^2 - t^2}}. \tag{3.19}$$

Formula (3.19) expresses the Radon transform of a radial function as a one-dimensional *integral transform*.

Our goal is the recovery of a function, f, from a knowledge of its Radon transform, $\mathcal{R}f$. Since $\mathcal{R}$ is a linear map, we might hope that there is a linear map $\mathcal{R}^{-1}$ from functions on $\mathbb{R} \times S^1$ to functions on $\mathbb{R}^2$ satisfying

$$\mathcal{R}^{-1} \circ \mathcal{R}f = f.$$

The inverse map should also be given by an integral formula. This turns out to be the case, but the derivation and analysis of this formula are rather involved. Because these spaces of functions are infinite dimensional, finding the inverse is not just a problem in linear algebra. The domain of $\mathcal{R}^{-1}$ is the range of $\mathcal{R}$, and neither the domain of $\mathcal{R}$ nor of $\mathcal{R}^{-1}$ is easy to describe explicitly. These issues are studied in Chapter 6. The remainder of this section is devoted to further properties of the Radon transform and its inverse.

Naively, we would expect that in order for $\mathcal{R}^{-1}$ to exist it would be necessary that $\mathcal{R}f(t, \boldsymbol{\omega}) = 0$ for all pairs $(t, \boldsymbol{\omega})$ only if $f \equiv 0$. In fact, it is easy to construct examples of functions that are not zero but have zero Radon transform.

***Example* 3.4.5.** Define the function

$$f(x, y) = \begin{cases} 1 & \text{if } (x, y) = (0, 0), \\ 0 & \text{if } (x, y) \neq (0, 0). \end{cases}$$

Clearly, $\mathcal{R}f(t, \boldsymbol{\omega}) = 0$ for all $(t, \boldsymbol{\omega})$.

From the point of view of measurement, this is a very trivial example. The next example is somewhat more interesting.

From "Introduction to the Mathematics of Medical Imaging, Second Edition" by Charles L. Epstein

Copyright ©2007 by the Society for Industrial and Applied Mathematics
This electronic version is for personal use and may not be duplicated or distributed.

***Example* 3.4.6.** Define a function f by setting $f(x, y) = 1$ if $x \in [-1, 1]$ and $y = 0$ and zero otherwise. Then $\mathcal{R}f(t, \boldsymbol{\omega}) = 0$ if $\boldsymbol{\omega} \neq (0, \pm 1)$ and $\mathcal{R}f(0, (0, \pm 1)) = 2$. In this case the Radon transform is usually zero, but for certain special lines it is not. Observe that if we replace f by a function $\tilde{f}$ that is 1 on some other subset of $\mathbb{R} \times 0$ of total length 2, then $\mathcal{R}f = \mathcal{R}\tilde{f}$. This gives examples, which are not entirely trivial, where the Radon transform does not contain enough information to distinguish between two functions.

The concept of a *set of measure zero* helps clarify these examples. We give a precise definition.

***Definition* 3.4.5.** A subset $E \subset \mathbb{R}^n$ is said to be of *n-dimensional measure zero* if for any $\epsilon > 0$ there is a collection of balls $B_{r_i}(\boldsymbol{x}_i)$ so that

$$E \subset \bigcup_{i=1}^{\infty} B_{r_i}(\boldsymbol{x}_i)$$

and

$$\sum_{i=1}^{\infty} r_i^n < \epsilon.$$

Such a set carries no n-dimensional mass.

For example, a point is set of measure zero in the line, a line is a set of measure zero in the plane, a plane is a set of measure zero in $\mathbb{R}^3$, and so on. From our perspective the basic fact about sets of measure zero is the following: If f is a function defined in $\mathbb{R}^n$ and the set of points where $f \neq 0$ is a set of measure zero, then [1]

$$\int_{\mathbb{R}^n} |f(\boldsymbol{x})|\, d\boldsymbol{x} = 0.$$

Indeed if φ is any function in $L^1(\mathbb{R}^n)$, then

$$\int_{\mathbb{R}^n} f(\boldsymbol{x})\varphi(\boldsymbol{x})\, d\boldsymbol{x} = 0.$$

As most linear models for realistic measurements are given by expressions of this sort, it follows that no practical measurement can distinguish such a function from the zero function.

Using the map $(t, \theta) \mapsto (t, \boldsymbol{\omega}(\theta))$, we can identify $\mathbb{R} \times [0, 2\pi)$ with $\mathbb{R} \times S^1$. A set in $\mathbb{R} \times S^1$ has measure zero if its preimage under this map does. With these concepts we can state a basic result about the Radon transform.

Proposition 3.4.2. *If f is a function defined in the plane supported on a set of measure zero, then the set of values $(t, \boldsymbol{\omega}) \in \mathbb{R} \times S^1$ for which $\mathcal{R}f(t, \boldsymbol{\omega}) \neq 0$ is itself a set of measure zero.*

[1] Strictly speaking, we should use the Lebesgue integral when discussing the integral of a function which is only nonzero on a set a measure zero. Such a function may fail to be Riemann integrable. See [43].

From "Introduction to the Mathematics of Medical Imaging, Second Edition" by Charles L. Epstein

Copyright ©2007 by the Society for Industrial and Applied Mathematics
This electronic version is for personal use and may not be duplicated or distributed.

As Example 3.4.6 shows, a function supported on a set of measure zero cannot, in general, be reconstructed from its Radon transform. Since the Radon transform is linear, it cannot distinguish functions which differ only on a set of measure zero. This is a feature common to any measurement process defined by integrals. While it is important to keep in mind, it does not lead to serious difficulties in medical imaging.

The support properties of f are reflected in the support properties of $\mathcal{R}f$.

Proposition 3.4.3. *Suppose that f is a function defined in the plane with $f(x, y) = 0$ if $x^2 + y^2 > R^2$. Then*

$$\mathcal{R}f(t, \boldsymbol{\omega}) = 0 \qquad \text{if } |t| > R. \tag{3.20}$$

Proof. Any line $l_{t,\boldsymbol{\omega}}$ with $|t| > R$ lies entirely outside of the support of f. From the definition it follows that $\mathcal{R}f(t, \boldsymbol{\omega}) = 0$ if $|t| > R$. □

If f is *known* to vanish outside a certain disk, then we do not need to compute its Radon transform for lines that are disjoint from the disk. It would be tempting to assert that the converse statement is also true, that is, "If $\mathcal{R}f(t, \boldsymbol{\omega}) = 0$ for $|t| > R$, then $f(x, y) = 0$ if $x^2 + y^2 > R^2$." As the next set of examples shows, this is false. We return to this question in Chapter 6.

***Example* 3.4.7.** For each integer $n > 1$ define a function, in polar coordinates, by setting

$$f_n(r, \theta) = r^{-n} \cos(n\theta).$$

These functions all blow up at $r = 0$ faster than r^{-1} and therefore do not belong to the natural domain of $\mathcal{R}$. This is because f_n cannot be integrated along any line that passes through $(0, 0)$. On the other hand, since f_n goes to zero as $r \to \infty$ like r^{-n} and $n > 1$, the integrals defining $\mathcal{R}f_n(t, \boldsymbol{\omega})$ converge absolutely for any $t \neq 0$. We use the following result:

***Lemma* 3.4.1.** *For each $n > 1$ and $t \neq 0, \boldsymbol{\omega} \in S^1$ the integrals*

$$\int_{l_{t,\boldsymbol{\omega}}} f_n(t\boldsymbol{\omega} + s\hat{\boldsymbol{\omega}})\, ds$$

converge absolutely and equal zero.

The proof of the lemma is at the end of this section. It already indicates the difficulty of inverting the Radon transform. These functions are not in the natural domain of the Radon transform because

$$\int_{-\infty}^{\infty} |f_n(-s \sin\theta, s \cos\theta)|\, ds = \infty$$

for any value of θ. On the other hand, $\mathcal{R}f_n(t, \boldsymbol{\omega}) = 0$ for all $t \neq 0$. So in some sense, $\mathcal{R}f_n$ is supported on the set of measure zero $\{0\} \times S^1$.

From "Introduction to the Mathematics of Medical Imaging, Second Edition" by Charles L. Epstein

Copyright ©2007 by the Society for Industrial and Applied Mathematics
This electronic version is for personal use and may not be duplicated or distributed.

For each n we modify f_n to obtain a function F_n in the natural domain of $\mathcal{R}$ such that $\mathcal{R}F_n(t,\boldsymbol{\omega}) = 0$ for all $(t,\boldsymbol{\omega})$, with $|t| > 1$. On the hand, the functions F_n do not vanish outside the disk or radius 1. The modified functions are defined by

$$F_n(r,\theta) = \begin{cases} f_n(r,\theta) & \text{for } r > 1, \\ 0 & \text{for } r \leq 1. \end{cases}$$

A line $l_{t,\boldsymbol{\omega}}$ with $|t| > 1$ lies entirely outside the unit disk. On such a line, the lemma applies to show that

$$\mathcal{R}F_n(t,\boldsymbol{\omega}) = \int\limits_{l_{t,\boldsymbol{\omega}}} f_n \, ds = 0.$$

On the other hand, F_n is bounded in a neighborhood of $(0,0)$ and therefore $\mathcal{R}F_n(t,\boldsymbol{\omega})$ is defined for all $(t,\boldsymbol{\omega}) \in \mathbb{R} \times S^1$. This shows that the Radon transform of a function may vanish for all t with $|t| > r$ without the function being zero outside disk of radius r.

Exercises

***Exercise* 3.4.1.** Provide a detailed proof for Proposition 3.4.1.

***Exercise* 3.4.2.** Find an explicit formula for the Radon transform of $\chi_{B_1(\boldsymbol{a})}$, for any $\boldsymbol{a} \in \mathbb{R}^2$.

***Exercise* 3.4.3.** Compute the Radon transform of $f(x,y) = xy\chi_{[-1,1]}(x)\chi_{[-1,1]}(y)$.

***Exercise* 3.4.4.** Let $f(x,y) = 1$ if $x^2 + y^2 = 1$ and zero otherwise. Show that $\mathcal{R}f(t,\boldsymbol{\omega}) = 0$ for all $(t,\boldsymbol{\omega}) \in \mathbb{R} \times S^1$.

***Exercise* 3.4.5.** Suppose that f and g are functions in the natural domain of the Radon transform. Show that if $f(\boldsymbol{x}) \geq g(\boldsymbol{x})$ for every $\boldsymbol{x} \in \mathbb{R}^2$, then

$$\mathcal{R}f(t,\boldsymbol{\omega}) \geq \mathcal{R}g(t,\boldsymbol{\omega}) \text{ for every } (t,\boldsymbol{\omega}) \in S^1 \times \mathbb{R}.$$

***Exercise* 3.4.6.** Suppose that f is a function defined on $\mathbb{R}^2$ such that the set of points where f is non-zero has measure zero. Show that if φ is a continuous function with bounded support, then

$$\int\limits_{-\infty}^{\infty} \mathcal{R}f(s,\boldsymbol{\omega})\varphi(t-s)\, ds = 0$$

for every t. Explain the relevance of this fact to medical imaging.

***Exercise* 3.4.7.** * Show that the set of points where $\chi_{\mathbb{Q}}$ is non-zero is a set of measure zero. Show that $\chi_{\mathbb{Q}}$ is *not* a Riemann integrable function.

***Exercise* 3.4.8.** Suppose that $\{\boldsymbol{x}_1, \ldots, \boldsymbol{x}_n\}$ are n distinct points on the unit circle. For $i \neq j$, let l_{ij} denote the line segment joining $\boldsymbol{x}_i$ to $\boldsymbol{x}_j$ and r_{ij} denote a real number. Show that if $r_{ij} = r_{ji}$ for all $i \neq j$, then there is function f supported on the line segments $\{l_{ij}\}$ such that

$$\int\limits_{l_{ij}} f\, ds = r_{ij} \text{ for all } i \neq j.$$

From "Introduction to the Mathematics of Medical Imaging, Second Edition" by Charles L. Epstein

Copyright ©2007 by the Society for Industrial and Applied Mathematics
This electronic version is for personal use and may not be duplicated or distributed.

***Exercise* 3.4.9.** Show that a line segment has measure zero as a subset of the plane.

***Exercise* 3.4.10.** Show that the x-axis has measure zero as a subset of the plane.

***Exercise* 3.4.11.** Show that the set $\{(0, \boldsymbol{\omega}) \ : \ \boldsymbol{\omega} \in S^1\}$ has measure zero as a subset of $\mathbb{R} \times S^1$.

3.4.1 Appendix: Proof of Lemma 3.4.1*

The proof of the theorem makes use of the elementary theory of complex variables and is not needed for the subsequent development of the book.

Proof. Let $z = x + iy$ and observe that by Euler's formula it follows that

$$f_n = \operatorname{Re} z^{-n}.$$

This means that for $t \neq 0$

$$\mathcal{R} f_n(t, \boldsymbol{\omega}) = \operatorname{Re} \int\limits_{l_{t,\boldsymbol{\omega}}} z^{-n}\, ds,$$

where ds is the arc element along the line. The line $(t, \boldsymbol{\omega}(\theta))$ can be represented as

$$z = (t + is)e^{i\theta}, \quad t \in \mathbb{R}.$$

Using this complex parameterization, the Radon transform of f_n can be reexpressed as a complex contour integral:

$$\mathcal{R} f_n(t, \theta) = \int\limits_{-\infty}^{\infty} f_n((t + is)e^{i\theta})\, ds = \operatorname{Re}\left[-ie^{-i\theta} \int\limits_{\operatorname{Re}(e^{-i\theta} z) = t} z^{-n}\, dz \right], \tag{3.21}$$

where the arc length element, along the line, is written in complex notation as

$$ds = -ie^{-i\theta} dz.$$

For $n > 1$ $\int z^{-n} = (1 - n)^{-1} z^{1-n}$; hence the theorem follows from (3.21). □

3.4.2 The Back-Projection Formula

Even though the line integrals of a function are concrete data, it is difficult to use these data directly to reconstruct the function. An obvious thing to try is averaging the values of the $\mathcal{R} f$ over the lines that pass through a point. For a direction $\boldsymbol{\omega}$, the line in the family $\{l_{t,\boldsymbol{\omega}} \ : \ t \in \mathbb{R}\}$, passing through a point $\boldsymbol{x}$ is given by $t = \langle \boldsymbol{x}, \boldsymbol{\omega} \rangle$. Thus we could try setting

$$\tilde{f}(\boldsymbol{x}) = \frac{1}{2\pi} \int\limits_0^{2\pi} \mathcal{R} f(\langle \boldsymbol{x}, \boldsymbol{\omega}(\theta) \rangle, \theta)\, d\theta. \tag{3.22}$$

This is called the *back-projection formula*. While it is a reasonable guess, it does not give the correct answer. Figure 3.10 shows the result of using back-projection to reconstruct a simple black and white image. The object is recognizable but blurry.

From "Introduction to the Mathematics of Medical Imaging, Second Edition" by Charles L. Epstein

Copyright ©2007 by the Society for Industrial and Applied Mathematics
This electronic version is for personal use and may not be duplicated or distributed.

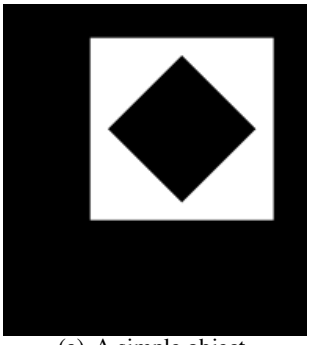

(a) A simple object.

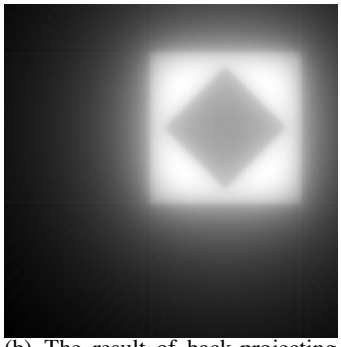

(b) The result of back-projecting the object's Radon transform.

Figure 3.10. Back-projection does not work.

To find the true inverse of the Radon transform requires an indirect approach passing through the Fourier transform. The Fourier transform, while perhaps more familiar, is a less transparent integral transform than the Radon transform. On the other hand, the inverse of the Fourier transform is easier to obtain. In the next chapter we consider the Fourier transform in some detail as it is of fundamental importance in the theory of image reconstruction and signal processing.

3.4.3 Continuity of the Radon Transform*

See: A.4.2, A.4.4.

The Radon transform is a linear transformation from functions defined in the plane to even functions on the space of lines. In medical applications, the function $\mathcal{R}f$ is an idealization for what is measured. Generally speaking, f is taken to be a bounded, though possibly discontinuous, function that vanishes outside of the patient. Suppose that f vanishes outside the disk of radius L and $f \leq M$. The lengths of the intersections of $l_{t,\boldsymbol{\omega}}$ with the support of f are bounded above $2L$, giving a crude estimate for $\mathcal{R}f$:

$$|\mathcal{R}f(t,\boldsymbol{\omega})| = \left| \int_{l_{t,\boldsymbol{\omega}}} f\, ds \right| \leq 2ML. \tag{3.23}$$

How sensitive are the measurements to errors? This is a question about the continuity properties of the map $f \mapsto \mathcal{R}f$. The answer to this question is important, but in the final analysis, it is not the correct question. What we really want to know is how sensitive the *reconstruction method* is to measurement errors. In other words, we want to understand the continuity properties of $\mathcal{R}^{-1}$. Since we have not yet constructed $\mathcal{R}^{-1}$, we consider the

Copyright ©2007 by the Society for Industrial and Applied Mathematics
This electronic version is for personal use and may not be duplicated or distributed.

somewhat easier question of the continuity of $\mathcal{R}$. That is, how sensitive are the measurements to the data? We need to choose a way to measure the size of the errors in both the data and the measurements. For the present we make the following choices: on the measurements we use the maximum of the integrals in the affine parameter

$$\| \mathcal{R}f(t,\boldsymbol{\omega})\|_{1,\infty} = \max_{\boldsymbol{\omega}\in S^1} \int_{-\infty}^{\infty} |\mathcal{R}f(t,\boldsymbol{\omega})|\, dt; \tag{3.24}$$

as a norm on the data we use the standard L^1-norm

$$\|f\|_1 = \int_{\mathbb{R}^2} |f(\boldsymbol{x})|\, d\boldsymbol{x}.$$

A function for which $\|f\|_1 < \infty$ is called an *absolutely integrable* or L^1-function. The set of such functions is denoted by $L^1(\mathbb{R}^2)$.

Proposition 3.4.4. *Suppose that f is an L^1-function in the natural domain of the Radon transform. Then*

$$\| \mathcal{R}f\|_{1,\infty} \leq \|f\|_1. \tag{3.25}$$

Proof. This proposition is a consequence of the triangle inequality, the change-of-variables formula, and the Fubini theorem. For each $\boldsymbol{\omega} \in S^1$ the triangle inequality implies that

$$\begin{aligned} \int_{-\infty}^{\infty} |\mathcal{R}f(t,\boldsymbol{\omega})|\, dt &\leq \int_{-\infty}^{\infty}\int_{-\infty}^{\infty} |f(t\boldsymbol{\omega} + s\hat{\boldsymbol{\omega}})|\, ds\, dt \\ &= \int_{\mathbb{R}^2} |f(x,y)|\, dx\, dy. \end{aligned} \tag{3.26}$$

In the second line we use the fact that $(s,t) \mapsto t\boldsymbol{\omega} + s\hat{\boldsymbol{\omega}}$ is an orthogonal change of variables. Since the last line is independent of $\boldsymbol{\omega}$, this proves the proposition. □

Because the Radon transform is linear this estimate implies that for any pair of functions, f, g, in the natural domain of $\mathcal{R}$, we have the estimate

$$\| \mathcal{R}f - \mathcal{R}g\|_{1,\infty} \leq \|f - g\|_1. \tag{3.27}$$

The fact that it takes time to make measurements means that, in the course of acquiring a full set of samples, the patient often moves. For a vector $\boldsymbol{\tau} = (\tau_1, \tau_2)$, let $f_{\boldsymbol{\tau}}$ denote the function f translated by the vector $\boldsymbol{\tau}$:

$$f_\tau(x,y) = f(x - \tau_1, y - \tau_2).$$

Suppose that we attempt to measure the $\mathcal{R}f(t,\boldsymbol{\omega})$ but the patient moves, a little, during the measurement process. A better model for what is measured is $\{\mathcal{R}f_{\boldsymbol{\tau}(\boldsymbol{\omega})}(t,\boldsymbol{\omega})\}$, where, as

From "Introduction to the Mathematics of Medical Imaging, Second Edition" by Charles L. Epstein

Copyright ©2007 by the Society for Industrial and Applied Mathematics
This electronic version is for personal use and may not be duplicated or distributed.

indicated, $\{\boldsymbol{\tau}(\boldsymbol{\omega})\}$ are vectors in $\mathbb{R}^2$ describing the position of the patient as a function of $\boldsymbol{\omega}$. The estimate (3.27) implies that

$$\|\mathcal{R}f - \mathcal{R}f_{\boldsymbol{\tau}}\|_{1,\infty} \leq \max_{\boldsymbol{\omega}\in S^1} \|f - f_{\boldsymbol{\tau}(\boldsymbol{\omega})}\|_1.$$

If *on average* f does not vary too quickly and the motions that arise are not too large then this estimate shows that the "actual" measurements $\{\mathcal{R}f_{\boldsymbol{\tau}(\boldsymbol{\omega})}(t,\boldsymbol{\omega})\}$ are close to the model measurements $\{\mathcal{R}f(t,\boldsymbol{\omega})\}$. Since the functions that arise in imaging are not continuous, it is important that while the average variation needs to be controlled, the pointwise variation does not. This is illustrated by an example.

***Example* 3.4.8.** Let $f(x,y) = \chi_{[-1,1]}(x)\chi_{[-1,1]}(y)$. If $\tau \neq 0$, then

$$\max_{\boldsymbol{x}} |f(\boldsymbol{x}) - f_{(\tau,0)}(\boldsymbol{x})| = 1.$$

On the other hand, for $|\tau| < 1$, it is also true that

$$\int_{\mathbb{R}^2} |f(\boldsymbol{x}) - f_{(0,\tau)}(\boldsymbol{x})|\, d\boldsymbol{x} = 4\tau.$$

Because of the averaging that occurs in the measurement process, it is often sufficient to keep the measurement errors small in a norm like $\|\cdot\|_{1,\infty}$. This fact is explained in Example 2.2.11.

As an application of functional analytic methods to the study of the Radon transform we show that the estimate (3.25) allows the extension of the Radon transform beyond its natural domain to $L^1(\mathbb{R}^2)$. To define this extension we observe that continuous functions with bounded support are dense in the space $L^1(\mathbb{R}^2)$. This means that for $f \in L^1(\mathbb{R}^2)$, we can choose a sequence $< f_n >$ of continuous functions, with bounded support so that

$$\lim_{n\to\infty} \|f - f_n\|_{L^1} = 0.$$

The Radon transform of f is the function on $\mathbb{R}\times S^1$ *defined* as the limit of the sequence of functions $< \mathcal{R}f_n >$ with respect to the L^1-norm. We let $\mathcal{R}f$ denote the limit. It also has the property that, for all $\boldsymbol{\omega} \in S^1$,

$$\int_{-\infty}^{\infty} |\mathcal{R}f(t,\boldsymbol{\omega})|\, dt \leq \|f\|_{L^1}.$$

On the other hand, $\mathcal{R}f$ is no longer given by the formula (3.12) as it is not known, a priori that these integrals converge. Fubini's theorem implies that these integrals are finite for almost every t.

From "Introduction to the Mathematics of Medical Imaging, Second Edition" by Charles L. Epstein

Copyright ©2007 by the Society for Industrial and Applied Mathematics
This electronic version is for personal use and may not be duplicated or distributed.

Exercises

***Exercise* 3.4.12.** Prove that the sequence of functions $< \mathcal{R} f_n >$ has a limit.

***Exercise* 3.4.13.** Compute the Radon transform of

$$f = \frac{\chi_{[0,1]}(x^2 + y^2)}{\sqrt{x^2 + y^2}}.$$

Is f in the natural domain of $\mathcal{R}$? What is $\| \mathcal{R} f \|_1$?

To close this chapter we study the Radon transform acting on radial functions. Inverting the transform in this case is simpler, reducing to a special case of the Abel transform.

3.5 The Radon Transform on Radial Functions

The Radon transform of a radial function does not depend on $\boldsymbol{\omega}$. It is given in (3.19) as an integral transform of a function of one variable. In this section, we suppress the dependence of the Radon transform on $\boldsymbol{\omega}$. After changing variables, we see that $\mathcal{R} f$ is a special case of an Abel transform. For $0 < \alpha \leq 1$, the *α-Abel transform* of g is defined by

$$\mathrm{A}_\alpha \, g(t) = \frac{1}{\Gamma(\alpha)} \int_t^\infty \frac{g(s)\, ds}{(s-t)^{1-\alpha}};$$

the coefficient $\Gamma(\alpha)$ is the *Gamma* function, defined in Section A.3.3. The theory of the Abel transform is outlined in Section 3.5.2. Among other things we show that

$$\mathrm{A}_{\frac{1}{2}}^{-1} = -\partial_t [\mathrm{A}_{\frac{1}{2}}]. \tag{3.28}$$

Suppose that $f(x, y) = F(\sqrt{x^2 + y^2})$; then changing variables shows that

$$\mathcal{R} f(t) = \sqrt{\pi} (\mathrm{A}_{\frac{1}{2}}(F_{\surd}))(t^2). \tag{3.29}$$

Here $F_{\surd}$ denotes the function $r \mapsto F(\sqrt{r})$. Using the formula for the inverse of the Abel transform (3.28) that is derived in Section 3.5.2 and a change of variables, we can solve equation (3.19) to obtain

$$F(r) = -\frac{1}{\pi r} \partial_r \left[\int_r^\infty \frac{\mathcal{R} f(t) t \, dt}{(t^2 - r^2)^{1/2}} \right]. \tag{3.30}$$

The inversion formula involves the Radon transform itself followed by a derivative. Differentiation is an unbounded operation, and this is where the subtlety in approximating the inverse of Radon transform lies. It is a consequence of (3.30) and Exercise 3.5.10 that a radial function f vanishes outside the disk of radius L if and only if $\mathcal{R} f(t) = 0$ for $|t| \geq L$.

From "Introduction to the Mathematics of Medical Imaging, Second Edition" by Charles L. Epstein

Copyright ©2007 by the Society for Industrial and Applied Mathematics
This electronic version is for personal use and may not be duplicated or distributed.

***Example* 3.5.1.** The characteristic function of an annular region,

$$\chi_{A_{ab}}(\boldsymbol{x}) = \chi_{[a^2,b^2]}(\|\boldsymbol{x}\|^2),$$

is a simple model for the sorts of functions encountered in medical imaging. It is piecewise differentiable with jump discontinuities. Using formula (3.19), we easily compute $\mathcal{R}\chi_{A_{ab}}$:

$$\mathcal{R}\chi_{A_{ab}}(t) = \begin{cases} 2[\sqrt{b^2 - t^2} - \sqrt{a^2 - t^2}] & \text{for } |t| \leq a, \\ 2\sqrt{b^2 - t^2} & \text{for } a < |t| \leq b, \\ 0 & \text{for } b < |t|. \end{cases} \tag{3.31}$$

Exercises

***Exercise* 3.5.1.** Prove formula (3.29).

***Exercise* 3.5.2.** Use formula (3.30) to compute the integrals

$$\int_r^1 \sqrt{\frac{1 - t^2}{t^2 - r^2}}\, t\, dt, \text{ for } 0 \leq r \leq 1.$$

***Exercise* 3.5.3.** Prove the formulæ in (3.31).

3.5.1 The Range of the Radial Radon Transform*

The remainder of this chapter is of a more advanced character, assuming some familiarity with elementary functional analysis. We study the Abel transforms and the range of the Radon transform on radial functions. The chapter concludes with an analysis of Volterra operators of the first kind. This is a class of operators which appear frequently in the study of inverse problems. The following notation is standard in functional analysis.

***Definition* 3.5.1.** The set of functions defined on $\mathbb{R}^n$ with k continuous derivatives is denoted $\mathcal{C}^k(\mathbb{R}^n)$.

Due to the simple structure of the inversion formula for radial functions, there are simple sufficient conditions for a function, ψ, to be the Radon transform of a bounded continuous, radial function. The next proposition is an example of such a result.

Proposition 3.5.1. *Let $\psi \in \mathcal{C}^2(\mathbb{R})$ satisfy the following conditions:*

1. $\psi(t) = \psi(-t)$.
2. *There is a constant M so that*

$$|\psi(t)| \leq M \text{ and } |\psi'(t)| \leq M.$$

3. *Both ψ and ψ' are absolutely integrable.*

From "Introduction to the Mathematics of Medical Imaging, Second Edition" by Charles L. Epstein

Copyright ©2007 by the Society for Industrial and Applied Mathematics
This electronic version is for personal use and may not be duplicated or distributed.

Then there is a bounded, continuous function $g(\boldsymbol{x}) = G(\|\boldsymbol{x}\|)$, in the natural domain of the Radon transform, such that

$$\mathcal{R}g = \psi.$$

Proof. For a function satisfying the preceding conditions we can integrate by parts to show that, for $r > 0$,

$$\tilde{g}(r) = \int_r^\infty \frac{\psi(t)t\,dt}{\sqrt{t^2 - r^2}} = -\int_r^\infty \psi'(t)\sqrt{t^2 - r^2}\,dt. \tag{3.32}$$

As both integrals have the same limit as r tends to 0, this identity holds for $r \geq 0$. It is not difficult to prove that $\tilde{g}$ is differentiable. Set

$$G(r) = -\frac{1}{\pi r}\partial_r \tilde{g}(r) = -\frac{1}{\pi}\int_r^\infty \frac{\psi'(t)\,dt}{\sqrt{t^2 - r^2}} \tag{3.33}$$

and $g(x, y) = G(\sqrt{x^2 + y^2})$.

To show that G is bounded, we split the integral into two parts. If $r \geq 1$, then

$$\begin{aligned} |G(r)| &\leq \frac{1}{\pi}\left[\int_r^{\sqrt{2}r} \frac{M\,dt}{\sqrt{t^2 - r^2}} + \frac{1}{r}\int_{\sqrt{2}r}^\infty |\psi'(t)|\,dt\right] \\ &\leq C\left[M + \int_0^\infty |\psi'(t)|\,dt\right]. \end{aligned} \tag{3.34}$$

If $r < 1$, a different argument is required. Because ψ is twice differentiable and even, there is a constant M' so that

$$|\psi'(t)| \leq M'|t|.$$

We then have the estimate

$$\begin{aligned} |G(r)| &\leq \frac{1}{\pi}\left[\int_r^1 \frac{M'|t|\,dt}{\sqrt{t^2 - r^2}} + \int_1^\infty |\psi'(t)|\,dt\right] \\ &\leq C'\left[M' + \int_0^\infty |\psi'(t)|\,dt\right]. \end{aligned} \tag{3.35}$$

The continuity of G is left as an exercise.

To show that g is absolutely integrable on lines, we interchange order of the integrations to obtain

$$\begin{aligned} \int_0^\infty |G(r)|\,dr &\leq \frac{1}{\pi}\int_0^\infty \int_0^t \frac{|\psi'(t)|\,dr\,dt}{\sqrt{t^2 - r^2}} \\ &= \frac{1}{2}\int_0^\infty |\psi'(t)|\,dt. \end{aligned} \tag{3.36}$$

From "Introduction to the Mathematics of Medical Imaging, Second Edition" by Charles L. Epstein

Copyright ©2007 by the Society for Industrial and Applied Mathematics
This electronic version is for personal use and may not be duplicated or distributed.

As $G(r)$ is bounded and absolutely integrable it follows that the integrals in (3.19), defining $\mathcal{R}g$, converge absolutely. It is now an elementary calculation to show that $\mathcal{R}G = \psi$. □

***Remark* 3.5.1.** Formula (3.33) gives an alternate form for the inverse of the Radon transform if $\mathcal{R}f$ satisfies the hypotheses of the proposition. A characterization of the range of the Radon transform similar to that in Proposition 3.5.1, though without the assumption of spherical symmetry, was already given by Radon.

Exercises

***Exercise* 3.5.4.** Prove that $\tilde{g}$, defined in (3.32), is a differentiable function.

***Exercise* 3.5.5.** Prove that $G(r)$ is a continuous function.

***Exercise* 3.5.6.** Prove the fact, used in (3.36), that

$$\int_0^t \frac{dr}{\sqrt{t^2 - r^2}} = \frac{\pi}{2}.$$

***Exercise* 3.5.7.** Give complete justifications for the statements that g is in the natural domain of the Radon transform and $\mathcal{R}g = \psi$.

3.5.2 The Abel Transform*

The Abel transform is a familiar feature of many problems involving measurement. It is also an important example of a nontrivial integral transform that nonetheless admits an explicit analysis. Formally, the inverse of the α-Abel transform is

$$\mathrm{A}_\alpha^{-1} = -\partial_x \mathrm{A}_{1-\alpha}. \tag{3.37}$$

This formula is a consequence of the identity

$$\int_x^s \frac{dt}{(t-x)^\alpha (s-t)^{1-\alpha}} = \Gamma(\alpha)\Gamma(1-\alpha), \tag{3.38}$$

which holds for $0 < \alpha < 1$. To derive the Abel inversion formula, we let

$$g(t) = \mathrm{A}_\alpha f = \frac{1}{\Gamma(\alpha)} \int_t^\infty \frac{f(s)\,ds}{(s-t)^{1-\alpha}}. \tag{3.39}$$

From "Introduction to the Mathematics of Medical Imaging, Second Edition" by Charles L. Epstein

Copyright ©2007 by the Society for Industrial and Applied Mathematics
This electronic version is for personal use and may not be duplicated or distributed.

Changing the order of the integration and using the preceding identity gives

$$\begin{aligned}\frac{1}{\Gamma(1-\alpha)}\int_x^\infty \frac{g(t)\,dt}{(t-x)^\alpha} &= \frac{1}{\Gamma(1-\alpha)\Gamma(\alpha)}\int_x^\infty\int_t^\infty \frac{f(s)\,ds\,dt}{(s-t)^{1-\alpha}(t-x)^\alpha}\\ &= \frac{1}{\Gamma(1-\alpha)\Gamma(\alpha)}\int_x^\infty\int_x^s \frac{f(s)\,dt\,ds}{(s-t)^{1-\alpha}(t-x)^\alpha}\\ &= \int_x^\infty f(s)\,ds.\end{aligned} \tag{3.40}$$

Taking the derivative, we obtain

$$f(x) = -\partial_x\left[\frac{1}{\Gamma(1-\alpha)}\int_x^\infty \frac{g(t)\,dt}{(t-x)^\alpha}\right]. \tag{3.41}$$

In other words,

$$I = -\partial_x \mathrm{A}_{1-\alpha}\circ \mathrm{A}_\alpha. \tag{3.42}$$

The operator $-\partial_x \mathrm{A}_{1-\alpha}$ is a *left inverse* to A_α.

Our derivation of the inversion formula is a formal computation, assuming that the various manipulations make sense for the given function f. The main points are the interchange of the order of integrations in the second line of (3.40) and the application of the fundamental theorem of calculus in (3.41). If f is continuous and absolutely integrable, then these steps are easily justified. For an L^1-function f, it follows that

$$\mathrm{A}_{1-\alpha}\circ \mathrm{A}_\alpha f = \int_x^\infty f(s)\,ds.$$

If f is also continuous, then this indefinite integral is differentiable and therefore

$$f = \partial_x \mathrm{A}_{1-\alpha}\circ \mathrm{A}_\alpha f.$$

It is not reasonable to use continuous functions to model the data of interest in medical imaging. Piecewise continuous functions provide a more accurate description. A piecewise continuous function of one variable can be represented as a sum

$$f(x) = f_c(x) + \sum_{j=1}^N \alpha_j \chi_{[a_j,b_j]}(x),$$

where $f_c(x)$ belongs to $\mathscr{C}^0(\mathbb{R})$, and the other term collects the jumps in f. As noted,

$$\mathrm{A}_{1-\alpha}\circ \mathrm{A}_\alpha \chi_{[a,b]}(x) = \int_x^\infty \chi_{[a,b]}(s)\,ds.$$

From "Introduction to the Mathematics of Medical Imaging, Second Edition" by Charles L. Epstein

Copyright ©2007 by the Society for Industrial and Applied Mathematics
This electronic version is for personal use and may not be duplicated or distributed.

If $x \neq a$ or b, then this function is differentiable with derivative 0 or 1. In order to interpret the formula at the exceptional points, we need to extend our notion of differentiability.

***Definition* 3.5.2.** A locally integrable function f has a *weak derivative* if there is a locally integrable function f_1 such that, for every continuously differentiable function, with bounded support g, the following identity holds:

$$\int_{-\infty}^{\infty} f(x)g'(x)\,dx = -\int_{-\infty}^{\infty} f_1(x)g(x)\,dx. \tag{3.43}$$

In this case f_1 is called the weak derivative of f.

If f is a differentiable function, then formula (3.43), with $f_1 = f'$, is just the usual integration by parts formula. The weak derivative of the indefinite integral of a piecewise continuous function is the function itself. This shows that the inversion formula, properly understood, is also valid for the sort of data that arise in imaging applications.

***Remark* 3.5.2.** Often the α-Abel transform is defined by

$$\mathcal{A}_\alpha f(t) = \frac{1}{\Gamma(\alpha)} \int_0^t \frac{f(s)\,ds}{(t-s)^{1-\alpha}}, \qquad \text{for } t \geq 0.$$

As before, α is in the interval $(0, 1]$. Using (3.38), we can show, at least formally, that

$$\mathcal{A}_\alpha^{-1} = \partial_x \mathcal{A}_{1-\alpha}. \tag{3.44}$$

The derivation of (3.44) is left as an exercise.

Exercises

***Exercise* 3.5.8.** Prove (3.38) by using the change of variables

$$t = \lambda x + (1-\lambda)s$$

and the classical formula

$$\int_0^1 \frac{d\lambda}{\lambda^\alpha (1-\lambda)^{1-\alpha}} = \Gamma(\alpha)\Gamma(1-\alpha);$$

see [130].

***Exercise* 3.5.9.** Let f be a piecewise continuous, L^1-function and $0 < \alpha \leq 1$. Show that if $\mathrm{A}_\alpha f(x) = 0$ for $x > R$, then $f(x) = 0$ for $x > R$ as well.

***Exercise* 3.5.10.** Use Exercise 3.5.9 to prove the following uniqueness result for the Radon transform. If f is a piecewise continuous, radial function in the natural domain of the Radon transform and $\mathcal{R}f(t) = 0$ for $|t| > R$, then $f(r) = 0$ if $r > R$.

From "Introduction to the Mathematics of Medical Imaging, Second Edition" by Charles L. Epstein

Copyright ©2007 by the Society for Industrial and Applied Mathematics
This electronic version is for personal use and may not be duplicated or distributed.

***Exercise* 3.5.11.** Generalize the argument given in (3.39)– (3.40) to prove that

$$\mathrm{A}_\alpha \circ \mathrm{A}_\beta = \mathrm{A}_{\alpha+\beta}\,.$$

For what range of α and β does this formula make sense?

***Exercise* 3.5.12.** For $0 < a < b$ compute $g_{a,b} = \mathrm{A}_\alpha(\chi_{[a,b]})$ and verify by explicit calculation that $\chi_{[a,b]}$ is the weak derivative of $-\mathrm{A}_{1-\alpha}(g_{a,b})$.

***Exercise* 3.5.13.** Provide the detailed justification for the derivation of (3.42) for f a continuous L^1-function.

***Exercise* 3.5.14.** Suppose that $f \in \mathscr{C}^1(\mathbb{R})$ and that f and f' are absolutely integrable. Show that

$$\mathrm{A}_\alpha\,[-\partial_x\,\mathrm{A}_{1-\alpha}]\,f = f.$$

***Exercise* 3.5.15.** Suppose that f is an L^1-function. Show that f is the weak derivative of

$$F(x) = -\int_x^\infty f(s)\,ds.$$

***Exercise* 3.5.16.** Derive the inversion formula (3.44) for the operator $\mathscr{A}_\alpha$. What hypotheses on f are needed to conclude that

$$\partial_x \mathscr{A}_{1-\alpha}(\mathscr{A}_\alpha f) = f?$$

How about

$$\mathscr{A}_\alpha(\partial_x \mathscr{A}_{1-\alpha} f) = f?$$

3.5.3 Volterra Equations of the First Kind*

See: A.2.6, A.6.2.

The Abel transforms are examples of a class of integral operators called Volterra operators. These operators are infinite-dimensional generalizations of upper triangular matrices. A linear transformation K is a Volterra operator of the first kind if it can be represented in the form

$$Kf(x) = \int_0^x k(x, y) f(y)\,dy.$$

This differs a little from the form of the Abel transform as the integral there extends from x to infinity, rather than 0 to x. The function $k(x, y)$ is called the *kernel function* of the integral operator K. The kernel functions for the Abel transforms are singular where $x = y$. In this section we restrict ourselves to kernel functions that satisfy an estimate of the form

$$|k(x, y)| \leq M,$$

From "Introduction to the Mathematics of Medical Imaging, Second Edition" by Charles L. Epstein

Copyright ©2007 by the Society for Industrial and Applied Mathematics
This electronic version is for personal use and may not be duplicated or distributed.

and analyze Volterra operators acting on functions defined on the interval [0, 1].

Volterra operators often appear in applications where one is required to solve an equation of the form

$$g = f + Kf = (\mathrm{Id} + K)f.$$

Such equations turn out to be easy to solve. Formally, we would write

$$f = (\mathrm{Id} + K)^{-1} g.$$

Still proceeding formally, we can express $(\mathrm{Id} + K)^{-1}$ as an infinite series:

$$(\mathrm{Id} + K)^{-1} f = \sum_{j=0}^{\infty} (-1)^j K^j f. \tag{3.45}$$

This is called the *Neumann series* for $(\mathrm{Id} + K)^{-1}$; it is obtained from the Taylor expansion of the function $(1 + x)^{-1}$ about $x = 0$:

$$(1 + x)^{-1} = \sum_{j=0}^{\infty} (-1)^j x^j.$$

Here $K^j f$ means the j-fold composition of K with itself. The sum on the right-hand side of (3.45) is an infinite sum of functions, and we need to understand in what sense it converges. That is, we need to choose a norm to measure the sizes of the terms in this sum. A useful property of Volterra operators is that this series converges for almost any reasonable choice of norm.

The basic estimates are summarized in the proposition.

Proposition 3.5.2. *Let* $1 \leq p \leq \infty$. *Suppose that* $|k(x, y)| \leq M$ *and* $f \in L^p([0, 1])$. *Then for* $x \in [0, 1]$ *and* $j \geq 1$

$$|K^j f(x)| \leq \frac{M^j x^{j-1}}{(j-1)!} \|f\|_{L^p}. \tag{3.46}$$

Proof. If $f \in L^p([0, 1])$ for a $p \geq 1$, then $f \in L^1([0, 1])$ and Hölder's inequality implies that

$$\|f\|_{L^1} \leq \|f\|_{L^p}.$$

In light of this, it suffices to prove (3.46) with $p = 1$. The proof is by induction on j. First consider $j = 1$:

$$\begin{aligned} |Kf(x)| &= \left| \int_0^x k(x, y) f(y)\, dy \right| \\ &\leq \int_0^x M |f(y)|\, dy \\ &\leq M \|f\|_{L^1}. \end{aligned} \tag{3.47}$$

From "Introduction to the Mathematics of Medical Imaging, Second Edition" by Charles L. Epstein

Copyright ©2007 by the Society for Industrial and Applied Mathematics
This electronic version is for personal use and may not be duplicated or distributed.

This verifies (3.46) for $j = 1$; assume it has been proved for j. Then

$$\begin{aligned} |K^{j+1} f(x)| &= \left| \int_0^x k(x, y) K^j f(y)\, dy \right| \\ &\leq \int_0^x M \frac{M^j y^{j-1}}{(j-1)!} \|f\|_{L^1}\, dy \\ &\leq \frac{M^{j+1} x^j}{j!} \|f\|_{L^1}. \end{aligned} \tag{3.48}$$

This completes the induction step and thereby the proof of the proposition. □

The proposition implies that $(\mathrm{Id}+K)^{-1} f - f$ converges pointwise uniformly, even if f is only in $L^p([0, 1])$. Indeed we have the pointwise estimate

$$|(\mathrm{Id}+K)^{-1} f(x) - f(x)| \leq M\|f\|_{L^1} \sum_{j=0}^{\infty} \frac{M^j x^j}{j!} = M\|f\|_{L^1} e^{Mx}. \tag{3.49}$$

Proposition 3.5.3. *If $f \in L^p([0, 1])$, then the equation $f = (\mathrm{Id}+K)g$ has a unique solution of the form $g = f + f_0$, where f_0 is a continuous function on $[0, 1]$ that satisfies the estimate*

$$|f_0(x)| \leq M\|f\|_{L^p} e^{Mx}.$$

In applications sometimes we encounter equations of the form

$$f = Kg, \tag{3.50}$$

where K is a Volterra operator of the first kind. A similar equation arose in the previous section. Provided that $k(x, y)$ is differentiable and $k(x, x)$ does not vanish, this sort of equation can be reduced to the type of equation considered in the last proposition. If (3.50) is solvable, then f must, in some sense, be differentiable. We formally differentiate equation (3.50) to obtain

$$f'(x) = k(x, x)g(x) + \int_0^x k_x(x, y)g(y)\, dy.$$

If K' denotes the Volterra operator with kernel function $k_x(x, y)/k(x, x)$, then this equation can be rewritten

$$\frac{f'(x)}{k(x, x)} = (\mathrm{Id}+K')g.$$

Applying our earlier result, we obtain the solution of the original equation in the form

$$g = (\mathrm{Id}+K')^{-1} \left(\frac{f'(x)}{k(x, x)} \right) = \left(\frac{f'(x)}{k(x, x)} \right) + \sum_{j=1}^{\infty} (-1)^j (K')^j \left(\frac{f'(x)}{k(x, x)} \right). \tag{3.51}$$

From "Introduction to the Mathematics of Medical Imaging, Second Edition" by Charles L. Epstein

Copyright ©2007 by the Society for Industrial and Applied Mathematics
This electronic version is for personal use and may not be duplicated or distributed.

In applications K describes a measurement process and f represents measurements. In this context it can be quite difficult to approximate f' accurately. As a result, it is often stated that a problem that involves solving an equation of the form (3.50) is *ill posed*. Small errors in measurement can lead to substantial errors in the solution of this type of equation. While it is reasonable to expect that we can control measurement errors in the sup norm, it is usually not possible to control errors in the derivatives of measurements, even in an L^p-norm. The inverse problem is ill posed because K^{-1} is not continuous as a map from $\mathscr{C}^0([0, 1])$ to itself.

***Remark* 3.5.3.** *Tikhonov regularization* provides a general method for finding approximate solutions to equation like (3.50), which is more stable than the exact solution. An exposition of this method can be found in [49]. The material in this section is a small sample from the highly developed field of integral equations. A good introductory treatment can be found in [131] or [106].

Exercises

***Exercise* 3.5.17.** Suppose that instead of assuming that $k(x, y)$ is uniformly bounded we assume that

$$\int_0^x |k(x, y)|^q \, dy \leq M$$

for a $1 < q < \infty$ and all $x \in [0, 1]$. Show that estimates analogous to (3.46) hold for $f \in L^p([0, 1])$, where $p = q(q - 1)^{-1}$.

***Exercise* 3.5.18.** Using the previous exercise, show that the equation $g = (\mathrm{Id} + K) f$ is solvable for $g \in L^p([0, 1])$.

***Exercise* 3.5.19.** Volterra operators of the first kind are infinite-dimensional generalizations of strictly upper triangular matrices. These are matrices a_{ij} such that $a_{ij} = 0$ if $i \leq j$. Suppose that A is an $n \times n$ strictly upper triangular matrix. Show that $A^n = 0$. Prove that $I + A$ is always invertible, and give a formula for its inverse.

3.6 Conclusion

The interaction of x-rays with matter is described, via Beer's law, in terms of the attenuation coefficient. The attenuation coefficient is a nonnegative function whose values reflect the internal structure of an object. In this chapter we have introduced a simple model for the measurements made in x-ray CT as the Radon transforms of the two-dimensional slices of the attenuation coefficient. As is typical of realistic measurement processes, the Radon transform is defined by an integral. As such it is not possible to distinguish functions that differ on very small sets, called sets of measure zero.

In the final sections we showed how to invert the Radon transform on radial functions. The inverse is the composition of an integral transform, essentially the Radon transform itself, *followed by* a derivative. While the inversion formula for radial functions is quite

From "Introduction to the Mathematics of Medical Imaging, Second Edition" by Charles L. Epstein

Copyright ©2007 by the Society for Industrial and Applied Mathematics
This electronic version is for personal use and may not be duplicated or distributed.

useful for working out simple examples and getting a feel for the Radon transform as mapping of infinite-dimensional spaces, it is not used in practical imaging applications. In the next several chapters we develop the mathematical tools needed to invert the Radon transform and process images in medical applications. The workhorse, throughout the subject, is the Fourier transform. In Chapter 6 we use the Fourier transform to derive a formula for the inverse of the Radon transform. This formula is the starting point for deriving the practical algorithms used in medical image reconstruction.

From "Introduction to the Mathematics of Medical Imaging, Second Edition" by Charles L. Epstein